Journal of Magnetic Resonance **155,** 236–243 (2002)
doi:10.1006/jmre.2002.2522, available online at http://www.idealibrary.com on IDEAL®

Tailored HCCH–TOCSY Experiment for Resonance Assignment in the Proximity of a Paramagnetic Center

Mario Piccioli[1] and Luisa Poggi

Magnetic Resonance Center, University of Florence, Via L. Sacconi 6, 50019 Sesto Fiorentino, Florence, Italy

Received July 31, 2001; revised December 10, 2001

The presence of a paramagnetic center may disturb both coherent and incoherent communication between nuclear spins that are affected, to some extent, by the hyperfine interaction. This is a limiting factor to an extensive use of paramagnetic probes in NMR spectroscopy to enhance partial alignment and to exploit cross correlation effects and pseudocontact shifts. We propose here an HCCH–TOCSY experiment tailored to identify spin systems involving resonances that are partly or completely affected by hyperfine interaction. The efficiency of polarization transfer steps when fast relaxing nuclei are involved is discussed. The sequence is tested for the protein Calbindin D_{9k}, in which one of the two native Ca^{2+} ions is replaced by the paramagnetic Ce^{3+} ion as well as for the oxidized form of cytochrome b_{562}.

Key Words: **HCCH–TOCSY; paramagnetic NMR; hyperfine interaction.**

INTRODUCTION

Paramagnetic centers in biomolecules induce contributions, often dominant, to shift and relaxation properties (*1*) of NMR signals, cause partial orientation due to their magnetic susceptibility anisotropy (*2, 3*), and provide cross correlation effects between Curie spin relaxation and dipole–dipole coupling (*2, 4–8*). As the latter are a potential source of additional structural information with respect to "classical" dipole–dipole and scalar couplings, the use of paramagnetic centers as probes to assess structural properties of biomolecules is quite fashionable in contemporary structural biology (*9–13*). On the other hand, the availability of additional information arising from the presence of a paramagnetic center is counterbalanced by the loss of information occurring in the proximity of the coordination sphere (*14, 15*). Since the detailed knowledge of metal environment is mandatory to achieve the complete understanding of the protein function, as well as to the exploitation of long range constraints arising from hyperfine interaction (*16*), it is necessary to develop experimental methods to assign resonances in the proximity of the metal ion. We report here a modified version of HCCH–TOCSY experiment, which has been tailored to this purpose. Although modifications discussed here do not substantially alter the coherence transfer pathway with respect to the scheme originally proposed by Kay and coworkers (*17*), they are mandatory in order to successfully exploit HCCH–TOCSY in the presence of contributions to relaxation arising from the hyperfine interaction.

Our interest to exploit feasibility of HCCH–TOCSY experiments in paramagnetic systems relies on the following reasons: (a) HCCH–TOCSY is one of the most widely used experiments to assign side chains in ^{13}C enriched proteins; (b) side chain assignment is particularly important in the case of metalloproteins, in which side chains of some amino acids bind the prosthetic group and may also play a crucial role in terms of catalysis and structure–function relationships (*18–20*).

When the prosthetic group is a paramagnet, the hyperfine interaction is transmitted, through contact contributions, to the side chains of metal bound residues. The latter are, within the entire protein frame, those that are most affected from the paramagnetic center (*13, 21–27*). It may therefore happen, as extensively reported in the literature, that a classical approach toward structure determination in a paramagnetic metalloprotein does not provide information in the proximity of the metal center (*28*), even when careful and extensive studies are performed using double and triple labeled samples (*29, 30*). Indeed, the partial or missing assignment of metal binding residues provides a lack of constraints in the region surrounding the prosthetic group (*31*). Therefore, a modified version of HCCH–TOCSY, which takes into account drawback arising from the hyperfine interaction, would be an excellent tool to identify resonances of side chains close to the metal center. The latter would provide the basis for identifying dipole–dipole connectivities and, therefore, to refine the structure also in the proximity of the paramagnetic center.

RESULTS AND DISCUSSION

The tailored version of the HCCH–TOCSY is reported in Fig. 1. The modifications that have been introduced with respect to the latest proposed version (*17*) of the experiment can be summarized as follows: (a) the transfer functions delays are suitably shortened; (b) the DIPSI sequence has been modified in order to be able to shorten the spin-lock time; (c) the flip back

[1] To whom correspondence should be addressed. E-mail: piccioli@cerm.unifi.it.

1090-7807/02 $35.00

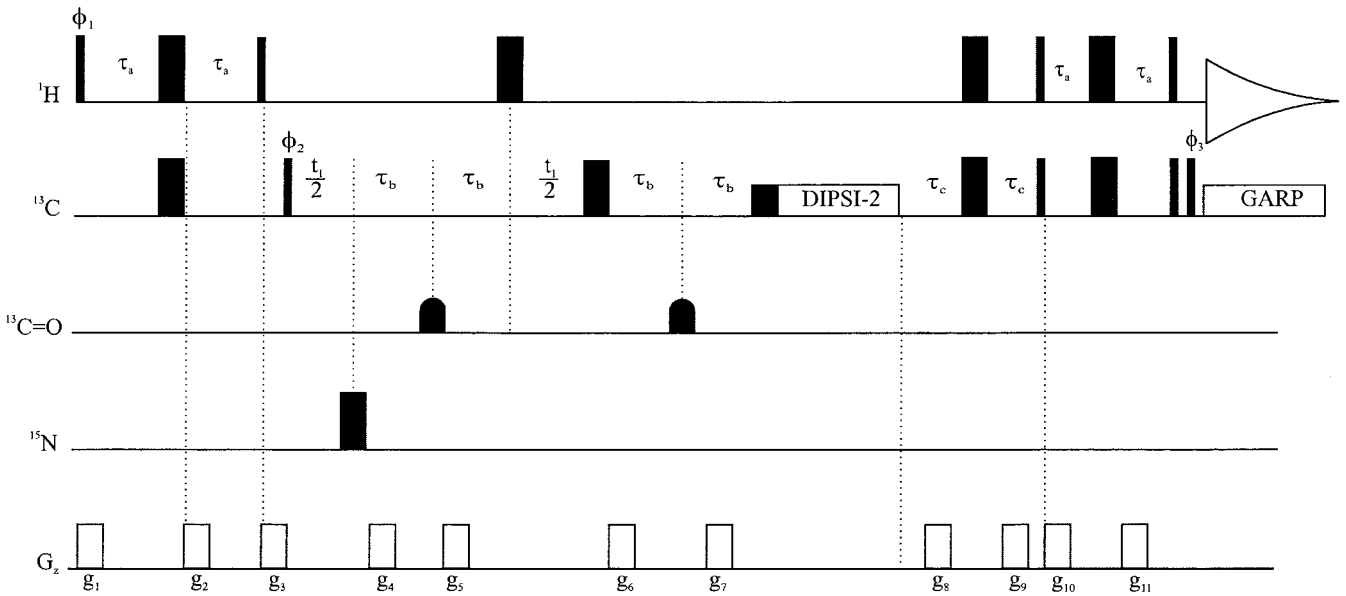

FIG. 1. Pulse scheme of the tailored HCCH–TOCSY sequence. All narrow (wide) pulses have flip angles of 90° (180°). The two C′ pulses are 180° pulses with a phase modulated shape profile. All the pulses of the DIPSI-2 sequence are applied along $\pm y$. The ^{13}C carrier is positioned at 39.8 ppm. The C′ 180° pulses are applied as phase-modulated pulses. Carbon decoupling during acquisition is achieved using the GARP decoupling sequence with a 3.5 kHz RF field. The values of τ_a, τ_b, and τ_c are 700, 475, and 500 μs, respectively. Mixing time and recycle delays of 2 and 100 ms, respectively, are employed. The duration and strengths of the gradients are $g_1 = g_2 = (300\ \mu s, 8\ G/cm)$; $g_3 = (475\ \mu s, 15\ G/cm)$; $g_4 = g_5 = g_6 = g_7 = (300\ \mu s, 4.8\ G/cm)$; $g_8 = g_9 = g_{10} = g_{11} = (300\ \mu s, 8\ G/cm)$. Tailored experiments were collected using a 1024×100 complex time domain matrix with acquisition times of 7.1 ms (t_1) and 28.5 ms (t_2). No water presaturation was used. All gradients are applied along the z axis and are rectangular. The phase cycle used is: $\phi_1 = x, -x$; $\phi_2 = 2(x), 2(-x)$; $\phi_3 = 4(x)$; rec $= x, -x, -x, x$. Quadrature detection in t_1 is obtained by States-TPPI (*47*) of ϕ_2.

pulses are eliminated, in order not to loose too much of information; (d) gradients are shortened; (e) recycle delay is shortened.

In principle, heteronuclear NMR is an excellent tool in paramagnetic systems (*14, 32*), because of the γ^2 dependency of hyperfine contribution to relaxation rates. The latter is much less effective when low γ nuclei are investigated (*26, 33–38*). Therefore, a critical step in HCCH–TOCSY, as well as in the other heterocorrelated experiments, is the polarization transfer between the high sensitivity ^{1}H nuclei and the low sensitivity ^{13}C nuclei. If we assume, as a rough approximation, that the antiphase magnetization H_xC_z relaxes as a function of ^{1}H T_2 and ^{13}C T_1, considering a CH pair in which proton and carbon are at the same distance from the metal ion, we observe that the relaxation is essentially dominated by the ^{1}H T_2 and hyperfine contributions effective on ^{13}C T_1 are almost negligible. This is shown in Fig. 2A, in which hyperfine contributions to longitudinal ^{1}H relaxation rates (R_{1p}) and to transverse ^{13}C relaxation rates (R_{2p}) are shown together with the relaxation-independent ^{1}H–^{13}C INEPT transfer function.

At increasing ^{1}H R_2 rates, the use of shorter INEPT transfer delays becomes mandatory in order to optimize the polarization transfer step. Figure 2B shows the need to optimize the INEPT transfer delay as a function of ^{1}H R_2 rates and sets the limit for the opportunity of polarization transfer based experiments vs direct excitation of the insensitive nucleus. When relaxation rates R_2 are larger than 1000 s^{-1}, the optimal delay for polarization transfer is 0.71 ms and it allows the transfer of 26% of the initial magnetization. This compensates for the sensitivity enhancements provided by polarization transfer, which depends on γ_H/γ_I ratio (*39*). Therefore, when lines larger than 400 Hz are involved, the use of polarization transfer as a first event in indirect detected experiment is not anymore recommended. Indeed, a direct excitation of the insensitive nuclei gives a stronger signal than what can be obtained by polarization transfer methods. In the case of NMR lines sharper than 400 Hz and affected by the hyperfine interaction, the INEPT transfer delay must be tuned to achieve the maximum of the relaxation-weighted transfer function.

Once H_xC_z coherence has been converted into H_zC_x, the lower gyromagnetic ratio of the ^{13}C nucleus protects coherence from paramagnetic relaxation. As shown in Fig. 2C, the effect of both ^{1}H R_{1p} and ^{13}C R_{2p} during the inverse INEPT step is almost negligible. On this basis, the shortening of the refocusing INEPT period is unlikely to significantly contribute to increase the observable signal. In the test case that we consider here, an hypothetical HC pair with both atoms at 4.0 Å from the metal ion would provide hyperfine contributions to relaxation of about 30 s^{-1} for both ^{13}C R_2 and ^{1}H R_1. This provides a decrease in the maximum of the transfer function smaller than 20% and a optimal transfer delay of 1.5 ms rather than 1.66 ms.

On the other hand, if longer delays are involved, also the hyperfine contribution to ^{13}C R_2 may become nonnegligible. This

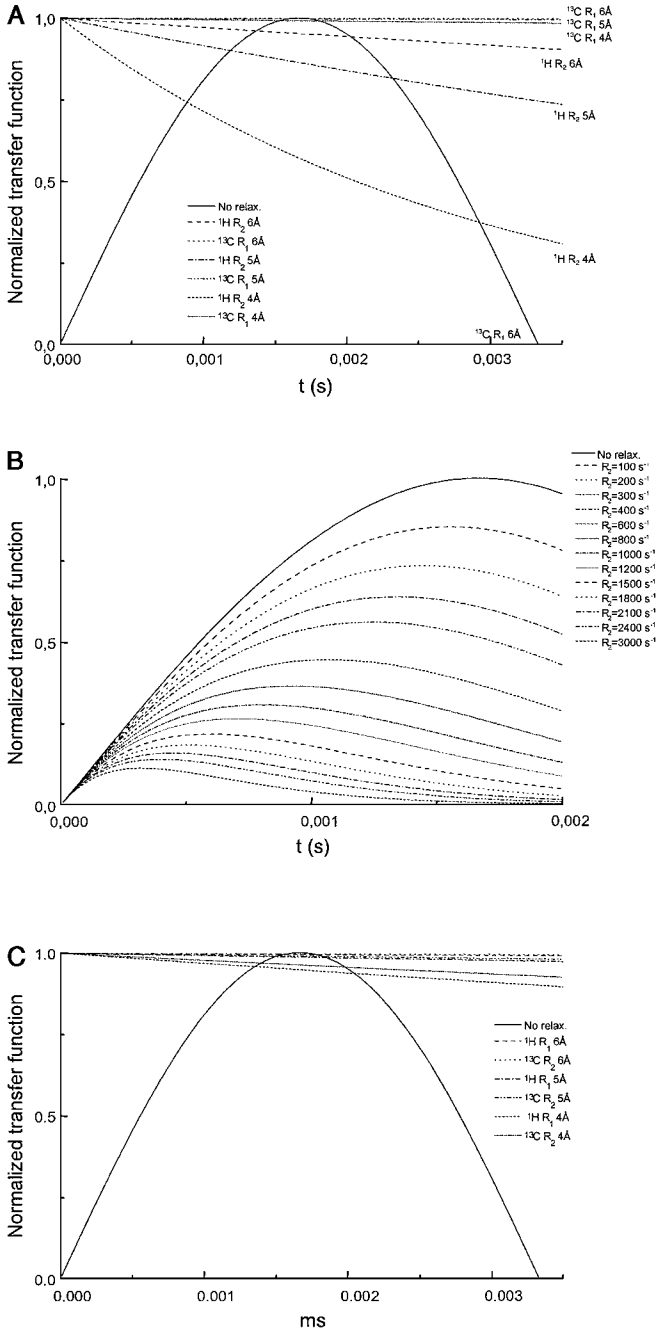

FIG. 2. (A) Hyperfine contributions to relaxation during a ^{1}H–^{13}C INEPT step as a function of the INEPT transfer delay, assuming that the antiphase magnetization H_xC_z relaxes as a sum of ^{1}H R_2 and ^{13}C R_1. The case of a CH pair in which proton and carbon are at the same distance from the metal ion is considered. The relaxation rates have been calculated considering contributions arising from electron nuclear dipole–dipole coupling and on the basis of the Solomon equation (*48*) and contributions arising from Curie spin relaxation (*49, 50*), assuming a system with $\tau_r = 4 \times 10^{-9}$ s, $\tau_r = 4 \times 10^{-13}$ s, an electronic spin $S = 5/2$, a magnetic field of 16.45 T (700 MHz proton Larmor frequency). The transfer function in the absence of relaxation is also reported. (B) Normalized magnetization transfer in a ^{1}H–^{13}C INEPT step as a function of the INEPT transfer delay at different ^{1}H R_2 rates. (C) Hyperfine contributions to relaxation rates in a ^{1}H–^{13}C inverse INEPT step as a function of relaxation rates assuming that the magnetization relaxes as a function of ^{1}H R_2 and ^{13}C R_1. Hyperfine relaxation rates have been calculated using the same parameters as for Fig. 2A.

is the case of the efficiency of the ^{13}C–^{13}C TOCSY transfer. The standard experimental conditions for a ^{13}C–^{13}C spin locked transfer imply 12–18 ms transfer time, typically corresponding to two or three loops of a DIPSI-3 scheme (*40*). Considering the same parameters used for the simulations in Fig. 2, the loss of signal intensity in the case of two ^{13}C signals occurring at 4 Å from a paramagnetic metal is more than 50%. Under these conditions, the spin locking sequence may become, in critical cases, a limiting factor. Indeed, if the standard DIPSI-3 sequence is used, the spin lock cannot be shortened below about 5 ms. Therefore, the replacement of DIPSI-3 with a DIPSI-2 sequence allows to easily achieve spin lock times as short as 2 ms. The use of short spin-lock times is often important to prevent complete signal loss during TOCSY transfer, in strict analogy with the homonuclear ^{1}H–^{1}H case (*41*).

The use of PFG within a pulse sequence to detect paramagnetic signals may be critical. Essentially, their use to clean observable magnetization from spurious peaks has no drawbacks, provided that PFG do not provide additional delays (*42*). Indeed, optimization of experimental delays, as in the case of INEPT transfer, may require gradients that are much shorter than "usual" gradient duration. On the other hand, the use of PFG for coherence selection, such as in echo-antiecho sequences or in some building blocks such as flip back or watergate schemes, lengthens the sequence thus decreasing the observable signal. Of course this effect depends on the duration of the inserted delays and on the relaxation mechanism that is operative during PFG. Use of PFG is critical when ^{1}H R_2 is involed. This is the case of echo–antiecho quadrature detection and, most importantly (even if this is not the case of this sequence), of watergate or water sculpting building blocks which therefore are not recommended in paramagnetic systems. Assuming that watergate sequence can be shortened down to 1.0 ms, a signal characterized by a linewidth of 200 Hz would loose half of its magnetization during the watergate scheme. If the same conditions of Fig. 2 are considered, this corresponds to a proton signal 3.6 Å away from the metal ion.

In the classical HCCH–TOCSY experiment (*17*), after the spin lock delay, the signal is converted into C_z magnetization and all magnetization left on the xy plane is then cleaned by a combination of gradients and trim pulses. Such efficient scheme may last for a few milliseconds and therefore result in an additional loss of observable magnetization. Therefore in the sequence tailored to paramagnetic signals we eliminated the flip back part. This results in a lower quality of water suppression which is, to a large extent, compensated by the use of fast recycle delays ensuring a progressive saturation of slow relaxing signals. Indeed, the adjustment of recycle delay is of paramount role: besides the effects of partial water suppression, the use of short recycle delays, which is made possible by the fast relaxation of the coherences of interests, may easily result in an increase in number of scans up to a factor of five. This contributes to increase the S/N ratio of fast relaxing signals that are usualy barely detectable from the noise.

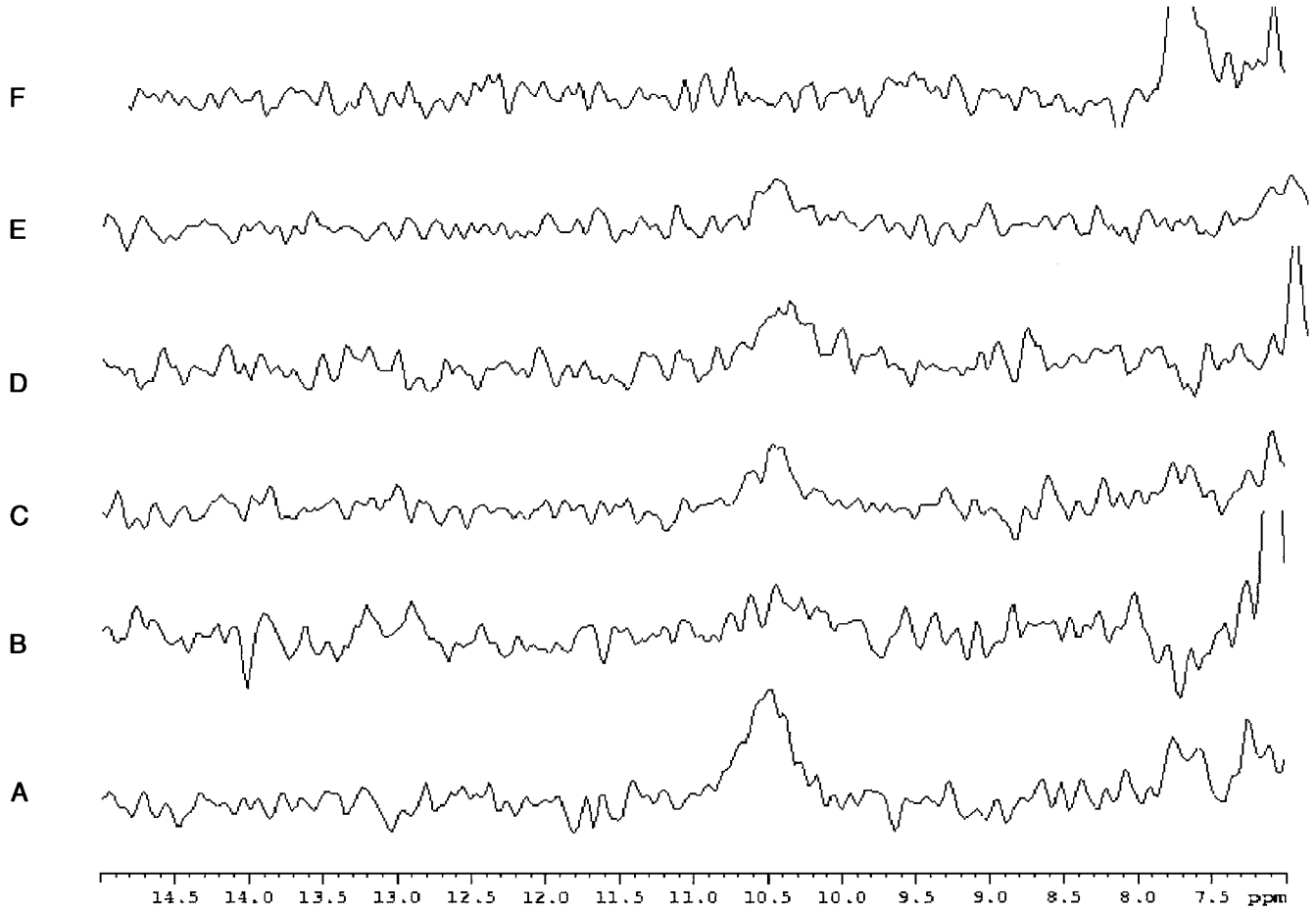

FIG. 3. Selected row HCCH–TOCSY experiment (47.1 ppm ^{13}C dimension) of the region corresponding to the H^{γ} signal of residue E65 (10.68 ppm). Spectra are acquired using different experimental conditions: (A) Tailored experiment, collected using parameters described in caption to Fig. 1; (B) Spectrum acquired using the standard sequence with diamagnetic delay for transfer functions, but with a recycle delay of 100 ms; (C) same as (A) but using a 5 ms spin-lock time, i.e., twice as long as in the tailored sequence; (D) same delays as in (A) and the flip-back pulses reintroduced in the tailored sequence; (E) same as (A) with a recycle delay of 600 ms instead of 100 ms. (F) Spectrum acquired using the standard pulse sequence. All experiments were collected on a 1.5 mM sample of ^{15}N, ^{13}C-labeled CaCe Calbindin D_{9k}, 90 : 10 H_2O/D_2O, pH 6.0, $T = 300$ K. Experiments were performed on a Bruker Avance 700 MHz spectrometer equipped with a TXI gradient probe and a gradient amplifier unit.

To quantify the effect of the proposed modifications on the signal-to-noise ratio of paramagnetic signals, we considered as a test sample the Calcium bindin protein Calbindin D_{9k}. The latter is a small (75 amino acids) protein containing two binding sites for Calcium in a classical EF hand type motif (*43*). As the two metal sites have different affinity for Ce(III) ions (and lanthanides in general), it is possible to selectively replace Ca(II) at Site II with paramagnetic Ce(III) (*44, 45*). This gives rise to a Ca–Ce derivative, in which all resonances in the environment of Ce(III) are affected by hyperfine interaction (*14*).

We recorded six spectra using different experimental conditions and we focused our attention on the most down-field shifted proton signal in the spectrum, corresponding to the C^{γ}/H^{γ} of E65 (10.68/47.1 ppm) (*14*). The carboxylate group of E65 side chain coordinates the Ce(III) ion and the H^{γ} proton signal at 10.68 ppm shows a linewidth of about 120 Hz.

Figure 3 shows the row corresponding to the E65 C^{γ}/H^{γ} peak under various experimental conditions. All of them are compared with the experiment fully tailored to detect paramagnetic signals, shown in Fig. 3A. First of all, we have acquired a spectrum using—in the modified version of the sequence shown in Fig. 1—the classic diamagnetic delays for coherence transfer, (τ_a, τ_b, τ_c of 1.6, 0.475, and 1.1 ms, respectively) but with a recycle delay of 100 ms (Fig. 3B), as used in the paramagnetic spectrum (Fig. 3A). The intensity of the signal of interest is scaled down by a factor of 4 with respect to the full paramagnetic version of the sequence. When the experiment is performed using a 5 ms spin-lock time, i.e., twice as long as the time shown in Fig. 3A, signal intensity is reduced by a factor of two (Fig. 3C). When the flip-back pulses are reintroduced in the tailored sequence, an approximately 30% decrease of the signal at 10.68 ppm is observed (Fig. 3D). The intensity

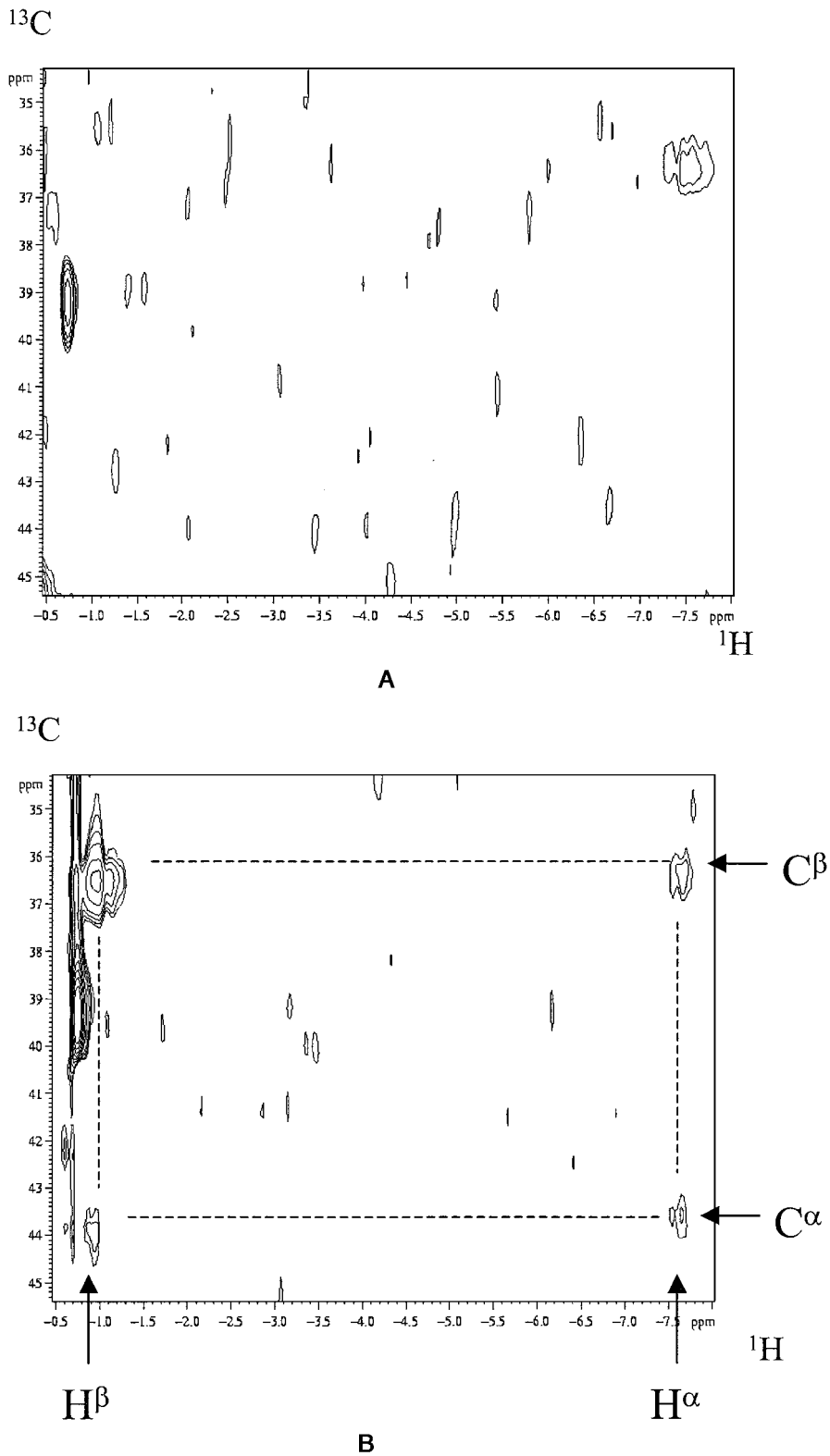

FIG. 4. (A) Expansion of the HCCH–TOCSY maps observed with the standard sequence. Only one clear connection between the H^{α} of D54 at −7.49 ppm and the C^{β} at 36.6 ppm is observed. (B) Expansion of the HCCH–TOCSY maps observed with the sequence and the parameters reported in Fig. 1. In this case, a complete coupling pattern involving D54 side chain is found. Experiments are performed on ^{15}N, ^{13}C-labeled CaCe Calbindin D_{9k}, same conditions as Fig. 3, on a Bruker Avance 700 MHz spectrometer.

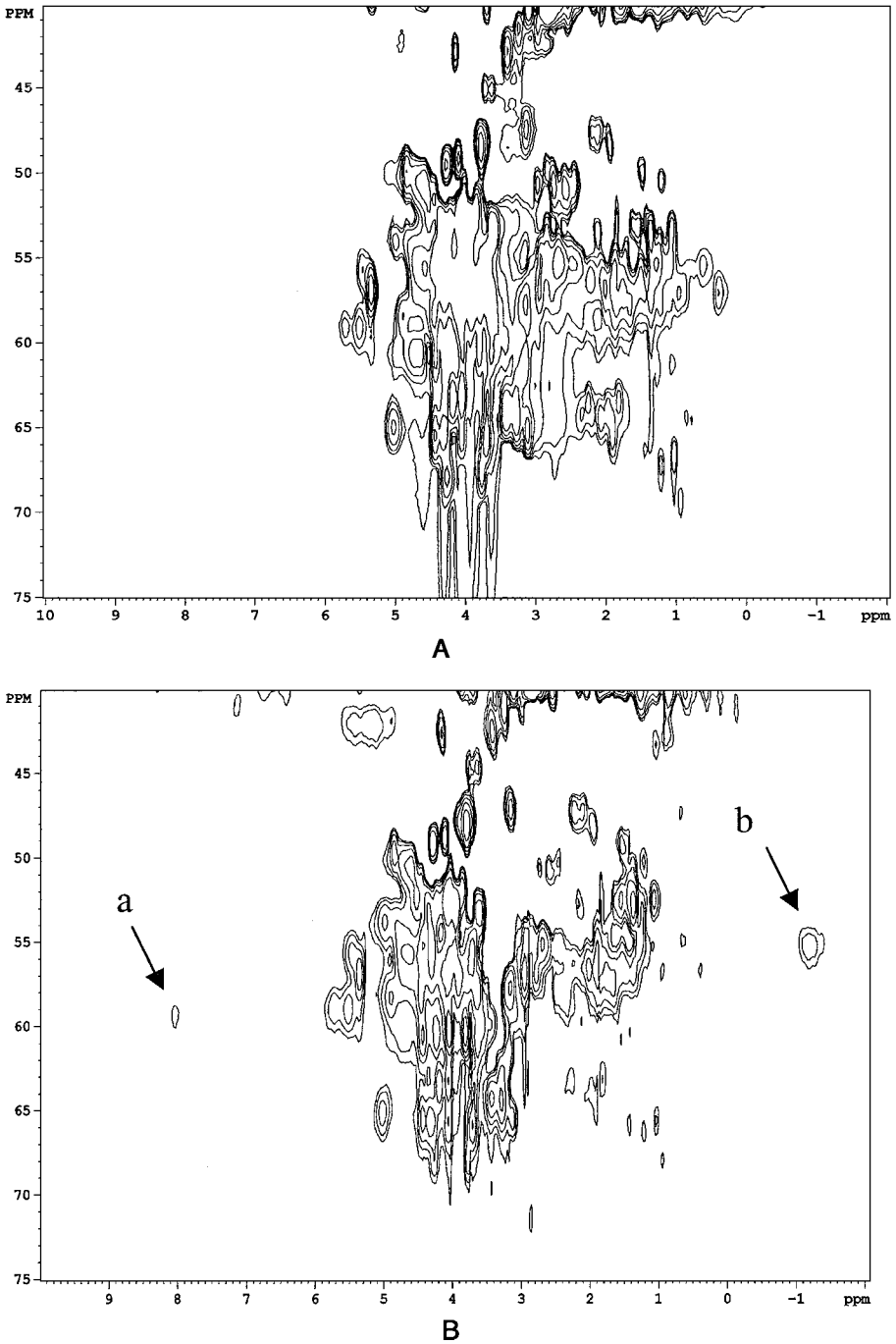

FIG. 5. (A) Expansion of the HCCH–TOCSY maps of oxidized Cytochrome b_{562} observed with the standard sequence. (B) Expansion of the HCCH–TOCSY maps observed with the sequence and the parameters reported in Fig. 1. Two additional peaks, are observed and indicated with arrows. They are tentatively assigned as the (a) Hα/Cα and (b) Hδ1/Cδ1 of the axial Histidine 102. Experiments are performed on ^{15}N, ^{13}C-labeled Cytochrome b_{562} (unlabeled heme), using the same conditions as Fig. 4, on a Bruker Avance 700 MHz spectrometer.

of the signal is scaled down by a factor of two also when using the tailored sequence with a recycle delay of 600 ms instead of 100 ms (Fig. 3E). To compare the two experiments with different recycle delays, we left the total experiment time unmodified.

The total effect of the modifications is therefore an increasing in the intensity of paramagnetic signals of, roughly, a factor of 25. As a consequence, the peak corresponding to the C^{γ}/H^{γ} correlation of E65 is not found at all in the spectrum acquired using the standard pulse sequence (Fig. 3F).

As a result, Fig. 4 shows a comparison of the two HCCH–TOCSY maps observed with the standard sequence and with the modified sequence. The region we observe involves signals in the region $0/-8$ ppm in the ^{1}H scale, whose chemical shifts clearly indicate the occurrence of contributions arising from the hyperfine interaction. Indeed, the signal at –7.5 ppm (ca. 200 Hz linewidth) has been already assigned to the H^{α} proton of D54, one of the residues which are bound to the Ce(III) ion via side chain carboxylate groups. While in the diamagnetic experiment (Fig. 4A) there is only one clear connection between the H^{α} of D54 at –7.49 ppm and the C^{β} at 36.6 ppm, a complete coupling pattern involving Asp 54 side chain is found only in the paramagnetic spectrum (Fig. 4B), which was obtained using the modified version of the classic HCCH–TOCSY sequence. In this way it is possible to clearly assign the resonances of H^{α}, H^{β}, C^{α}, and C^{β} of D54.

In order to provide further evidence of the efficiency of this pulse sequence, the tailored HCCH–TOCSY was also applied on cytochrome b_{562} in the oxidized form. The latter is a paramagnetic protein extensively characterized by NMR (*46*). Figure 5 shows the comparison of two HCCH–TOCSY maps analogous to the case shown in Fig. 4. Two additional peaks are clearly observed when the spectrum is acquired using the modified sequence (Fig. 5B). They correspond to two ^{1}H resonances unassigned in previous studies. Although their assignment is beyond the scope of the present article, the analysis of hyperfine shifts and the inspections of the assignments already available (*46*) suggest that H^{α}/C^{α} and $H^{\delta 2}/C^{\delta 2}$ of His 102, the axial histidine in the heme pocket, are the most likely candidates for the observed resonances.

CONCLUSIONS

We have shown that, although the hyperfine interaction disturbs coherent and incoherent communications between nuclei, the transfer of magnetization to low γ nuclei attenuates the effects of hyperfine relaxation and allows not only the direct observation and identification of nuclei at very short distances from the metal center, but also the detection of coherence transfer pathways from such nuclei. The availability of an HCCH–TOCSY experiment optimized to identify coherence pathways involving signals affected by hyperfine relaxation is a relevant issue due to the structural and biological features of metalloproteins. The knowledge of the structure in solution of the first coordination sphere and of the active site is often essential to the understanding of structure–function relationships in such systems. The tailored HCCH–TOCSY sequence that we presented here may result in a net gain of signal intensity for signals affected by hyperfine interaction of about two orders of magnitude with respect to the standard sequence. The use of HCCH–TOCSY experiments to assign side chains of metal bound residues will be an important issue to obtain safer and faster assignments in the proximity of a paramagnetic center.

ACKNOWLEDGMENTS

We are grateful to Profs. I. Bertini and C. Luchinat for encouraging this work and to Dr. Y. M. Lee for providing us with the CaCe Calbindin D9k sample. This work was supported by CNR Progetto Finalizzato Biotecnologie (99.00509.PF49), by MURST Progetto Ex 40%, and by the European Union RTD Project "Find Structure" QLG2-1999-01003.

REFERENCES

1. I. Bertini and C. Luchinat, "NMR of Paramagnetic Substances," Coord. Chem. Rev., Vol. 150, Elsevier, Amsterdam (1996).
2. J. R. Tolman, J. M. Flanagan, M. A. Kennedy, and J. H. Prestegard, Nuclear magnetic dipole interactions in field-oriented proteins: information for structure determination in solution, *Proc. Natl. Acad. Sci. USA* **92,** 9279–9283 (1995).
3. L. Banci, I. Bertini, J. G. Huber, C. Luchinat, and A. Rosato, Partial orientation of oxidized and reduced cytochrome b_5 at high magnetic fields: Magnetic susceptibility anisotropy contributions and consequences for protein solution structure determination, *J. Am. Chem. Soc.* **120,** 12,903–12,909 (1998).
4. I. Bertini, C. Luchinat, and D. Tarchi, Are true scalar proton–proton connectivities ever measured in COSY spectra of paramagnetic macromolecules?, *Chem. Phys. Lett.* **203,** 445–449 (1993).
5. I. Bertini, C. Luchinat, M. Piccioli, and D. Tarchi, COSY spectra of paramagnetic macromolecules, observability, scalar effects, cross correlation effects, relaxation allowed coherence transfer, *Concepts Magn. Reson.* **6,** 307–335 (1994).
6. R. Ghose and J. H. Prestegard, Electron spin-nuclear spin cross-correlation effects on multiplet splittings in paramagnetic proteins, *J. Magn. Reson.* **128,** 138–143 (1997).
7. J. C. Hus, D. Marion, and M. Blackledge, De novo determination of protein structure by NMR using orientational and long-range order restraints, *J. Mol. Biol.* **298,** 927–936 (2000).
8. J. Boisbouvier, P. Gans, M. Blackledge, B. Brutscher, and D. Marion, Long-range structral information in NMR studies of paramagnetic molecules from electron spin-nuclear spin cross-correlated relaxation, *J. Am. Chem. Soc.* **121,** 7700–7701 (1999).
9. M. A. Contreras, J. Ubach, O. Millet, J. Rizo, and M. Pons, Measurement of one bond dipolar couplings through lanthanide-induced orientation of a calcium-binding protein, *J. Am. Chem. Soc.* **121,** 8947–8948 (1999).
10. N. V. Shokhirev, T. K. Shokhireva, J. R. Polam, C. T. Watson, K. Raffii, U. Simonis, and F. A. Walker, *J. Phys. Chem.* **101,** 2778 (1997).
11. R. R. Biekofsky, S. R. Martin, J. P. Browne, P. M. Bayley, and J. Feeney, Ca^{2+} coordination to backbone carbonyl oxygen atoms in Calmodulin and other EF-hand proteins: ^{15}N chemical shifts as probes for monitoring individual-site Ca^{2+} coordination, *Biochemistry* **37,** 7617–7629 (1998).
12. R. R. Biekofsky, F. W. Muskett, J. M. Schmidt, S. R. Martin, J. P. Browne, P. M. Bayley, and J. Feeney, NMR approaches for monitoring domain orientations in calcium-binding proteins in solution using partial replacement of Ca^{2+} by Tb^{3+}, *FEBS Lett.* **460,** 519–526 (1999).
13. F. Arnesano, L. Banci, I. Bertini, K. van der Wetering, M. Czisch, and R. Kaptein, The auto-orientation in high magnetic field of oxidized cytochrome b_{562} as source of constraints for solution structure determination, *J. Biomol. NMR* **17,** 295–304 (2000).
14. I. Bertini, Y.-M. Lee, C. Luchinat, M. Piccioli, and L. Poggi, Locating the metal ion in calcium-binding proteins by using Cerium(III) as a probe. *ChemBioChem* **2,** 550–558 (2001).

15. I. Bertini, A. Donaire, C. Luchinat, B. Jimenez, G. Parigi, M. Piccioli, and L. Poggi, The refinement of solution structure of Calbindin D9k: Assessment of various constraints for structure calculations, *J. Biomol. NMR* **21,** 85–98 (2001).

16. I. Bertini, C. Luchinat, and M. Piccioli, Paramagnetic probes in metalloproteins. Turning limitations into advantages, *Methods Enzymol.* **339,** 314–340 (2001).

17. L. E. Kay, G. Y. Xu, A. U. Singer, D. R. Muhandiram, and J. D. Forman-Kay, A gradient-enhanced HCCH–TOCSY experiment for recording side-chains ^{1}H and ^{13}C correlations in H_2O samples of proteins, *J. Magn. Reson. Ser. B* **101,** 333–337 (1993).

18. "Physical Methods in Bioinorganic Chemistry: Spectroscopy and Magnetism," University Science Books, Sausalito, CA (2000).

19. I. Bertini, H. B. Gray, S. J. Lippard, J. S. Valentine, and Eds., "Bioinorganic Chemistry," University Science Books, Mill Valley, CA (1994).

20. J. A. Cowan, "Inorganic Biochemistry: An Introduction," VCH, Weinheim (1993).

21. I. Bertini, P. Turano, and A. J. Vila, NMR of paramagnetic metalloproteins, *Chem. Rev.* **93,** 2833–2932 (1993).

22. A. J. Vila and C. O. Fernández, The structure of the metal site in *Rhus vernicifera* stellacyanin: A paramagnetic NMR study on its Co(II)-derivative, *J. Am. Chem. Soc.* **118,** 7291–7298 (1996).

23. A. J. Vila, B. E. Ramirez, A. J. Di Bilio, T. J. Mizoguchi, J. H. Richards, and H. B. Gray, Paramagnetic NMR spectroscopy of Co(II) and Cu(II) derivatives of pseudomonas aeruginosa His46Asp azurin, *Inorg. Chem.* **36,** 4567–4570 (1997).

24. I. Bertini, S. Ciurli, A. Dikiy, C. O. Fernández, C. Luchinat, N. Safarov, S. Shumilin, and A. J. Vila, *J. Am. Chem. Soc.* **123,** 2405–2413 (2001).

25. R. O. Louro, I. J. Correia, L. Brennan, I. B. Coutinho, A. V. Xavier, and D. L. Turner, Electronic structure of low-spin ferric porphyrins: ^{13}C NMR studies of the influence of axial ligand orientation, *J. Am. Chem. Soc.* **120,** 13,240–13,247 (1998).

26. U. Kolczak, J. Salgado, G. Siegal, M. Saraste, and G. W. Canters, Paramagnetic NMR studies of blue and purple copper proteins, *Biospectroscopy* **5,** S19–S32 (1999).

27. J. Salgado, A. P. Kalverda, R. E. Diederix, G. W. Canters, J. M. Moratal, A. T. Lawler, and C. Dennison, Paramagnetic NMR investigations of Co(II) and Ni(II) amicyanin, *JBIC* **4,** 457–467 (1999).

28. S. S. Pochapsky, N. U. Jain, M. Kuti, T. A. Lyons, and J. Heymont, A refined model for the solution structure of oxidized putidaredoxin, *Biochemistry* 4681–4690 (1999).

29. S. Vathyam, R. A. Byrd, and A. F. Miller, Assignment of the backbone resonances of oxidized Fe-superoxide dismutase, a 42 kDa paramagnet-containing enzyme, *J. Biomol. NMR* **14,** 293–294 (1999).

30. S. Vathyam, R. A. Byrd, and A. F. Miller, Mapping the effects of metal ion reduction and substrate analog binding to Fe-superoxide dismutase by NMR spectroscopy, *Magn. Reson. Chem.* **38,** 536–542 (2000).

31. A. M. Prantner, B. F. Volkman, S. J. Wilkens, B. Xia, and J. L. Markley, Assignment for ^{1}H, ^{13}C, and ^{15}N signals of reduced *Clostridium pasteurianum* rubredoxin: Oxidation state-dependent changes in chemical shifts and relaxation rates, *J. Biomol. NMR* **10,** 411–412 (1997).

32. I. Bertini, C. Luchinat, R. Macinai, M. Piccioli, A. Scozzafava, and M. S. Viezzoli, Paramagnetic metal centers in proteins can be investigated through heterocorrelated NMR spectroscopy, *J. Magn. Reson. Ser. B* **104,** 95–98 (1994).

33. J. A. R. Worrall, U. Kolczak, G. W. Canters, and M. Ubbink, Interaction of yeast iso-1-cytochrome c with Cytochrome c Peroxidase investigated by [^{15}N,^{1}H] heteronuclear NMR spectroscopy, *Biochemistry* **40,** 7069–7076 (2001).

34. M. Ubbink, L. Y. Lian, S. Modi, P. A. Evans, and D. S. Bendall, *Eur. J. Biochem.* **242,** 132–147 (1996).

35. Y. K. Chae and J. L. Markley, Analysis of teh hyperfine-shifted nitrogen-15 resonances of the oxidized form of *Anabena 7120* heterocyst ferredoxin, *Biochemistry* **34,** 188–193 (1995).

36. B. Xia, W. M. Westler, H. Cheng, J. Meyer, J.-M. Moulis, and J. L. Markley, Detection and classification of hyperfine-shifted 1H, 2H, and 15N resonances from the four cysteines that ligate iron in oxidized and reduced *Clostridium pasteurianum* rubredoxin, *J. Am. Chem. Soc.* **117,** 5347–5350 (1995).

37. J. Boyd, C. M. Dobson, A. S. Morar, R. J. P. Williams, and G. J. Pielak, ^{1}H and ^{15}N hyperfine shifts of cytochrome c, *J. Am. Chem. Soc.* **121,** 9247–9248 (1999).

38. R. D. Guiles, V. J. Basus, S. Sarma, S. Malpure, K. M. Fox, I. D. Kuntz, and L. Waskell, Novel heteronuclear methods of assignment transfer from a diamagnetic to a paramagnetic protein: Application to rat cytochrome b5, *Biochemistry* **32,** 8329–8340 (1993).

39. G. Bodenhausen and D. J. Ruben, Natural abundance nitrogen-15 NMR by enhanced heteronuclear spectroscopy, *Chem. Phys. Lett.* **69,** 185–188 (1980).

40. A. J. Shaka, C. J. Lee, and A. Pines, Iterative schemes for bilinear operators: Application to spin decoupling, *J. Magn. Reson.* **77,** 274–293 (1988).

41. M. Sadek, R. T. C. Brownlee, S. D. B. Scrofani, and A. G. Wedd, TOCSY assignment of broad resonances in paramagnetic proteins, *J. Magn. Reson.* **101,** 309–314 (1993).

42. K. Skidmore and U. Simonis, Novel strategy for assigning hyperfine shifts using pulsed-field gradients heteronuclear multiple-bond correlation spectroscopy, *Inorg. Chem.* **35,** 7470–7471 (1996).

43. L. A. Svensson, E. Thulin, and S. Forsén, Proline cis-trans isomers in calbindin D_{9k} observedby X-ray crystllography, *J. Mol. Biol.* **223,** 601–606 (1992).

44. M. Akke, S. Forsén, and W. J. Chazin, Molecular basis for co-operativity in Ca^{2+} binding to calbindin D_{9k}. ^{1}H nuclear magnetic resonance studies of (Cd^{2+})1-bovine calbindin D_{9k}., *J. Mol. Biol.* **220,** 173–189 (1991).

45. H. J. Vogel, T. Drakenberg, S. Forsén, J. D. O'Neil, and T. Hofmann, Structural differences in the two calcium binding sites of the porcine intestinal calcium binding protein: A multinuclear NMR study, *Biochemistry* **24,** 3870–3876 (1985).

46. F. Arnesano, L. Banci, I. Bertini, J. Faraone-Mennella, A. Rosato, P. D. Barker, and A. R. Fersht, The solution structure of oxidized e*scherichia coli* cytochrome b_{562}, *Biochemistry* **38,** 8657–8670 (1999).

47. D. Marion, M. Ikura, R. Tschudin, and A. Bax, Rapid recording of 2D NMR spectra without phase cycling. Application to the study of hydrogen exchange in proteins, *J. Magn. Reson.* **85,** 393–399 (1989).

48. I. Solomon and N. Bloembergen, Nuclear magnetic interactions in the HF molecule, *J. Chem. Phys.* **25,** 261–266 (1956).

49. M. Guéron, Nuclear relaxation in macromolecules by paramagnetic ions: A novel mechanism, *J. Magn. Reson.* **19,** 58–66 (1975).

50. A. J. Vega and D. Fiat, Nuclear relaxation processes of paramagnetic complexes. The slow motion case, *Mol. Phys.* **31,** 347–355 (1976).